

multi-Risk sciEnce for resilientT commUnities undeR a changiNg climate

Codice progetto MUR: **PE00000005** – F83C22001660002



Deliverable title: Procedure for nanoparticles tracking

Deliverable ID: DV 4.5.1

Due date: 31/03/2026

Submission date: 16/02/2026

AUTHORS

**Rajandrea Sethi (PoliTO), Silvia Lupato (PoliTO); Monica Granetto (PoliTO);
Martco Coha (PoliTO); Alessandro Casasso (PoliTO); Laura Riva (POLIMI);
Carlo Punta (POLIMI)**



1. Technical references

Project Acronym	RETURN
Project Title	multi-Risk sciEnce for resilientT commUnities undeR a changiNg climate
Project Coordinator	Domenico Calcaterra UNIVERSITA DEGLI STUDI DI NAPOLI FEDERICO II domcalca@unina.it
Project Duration	December 2022 – November 2025 (36 months)
Deliverable No.	DV4.5.1
Dissemination level*	PP
Work Package	WP5 - WP Title: Prevention and remediation
Task	T4.5.1 - Task Title: Sensing and/or removal of contaminants with physical-chemical and electrochemical processes
Lead beneficiary	UNIPA & UNICA
Contributing beneficiary/ies	PoliTO, POLIMI

* PU = Public

PP = Restricted to other programme participants (including the Commission Services)

RE = Restricted to a group specified by the consortium (including the Commission Services)

CO = Confidential, only for members of the consortium (including the Commission Services)

Document history

Version	Date	Lead contributor	Description
0.1	21-11-2025	Rajandrea Sethi (PoliTO), Laura Riva (POLIMI) and Carlo Punta (POLIMI)	Individual contributions to the First draft
0.2	16-02-2026	Daniele Di Trapani (UNIPA) and Carlo Punta (PoliMI) – Task Coordinators, and Laura Riva	First draft
0.3			Edits for approval
1.0			Final version



2. Abstract

Performing nanoparticle transport tests is crucial for developing effective nanoremediation strategies, as these tests provide valuable insights into the behavior and mobility of nanoparticles in subsurface environments. Transport tests provide critical data on how nanoparticles interact with the medium, including attachment, detachment, and deposition mechanisms. This information is key to predicting nanoparticle fate and transport under real-world conditions and tailoring formulations for site-specific applications.

The tests allow fine-tuning the injection parameters, such as flow rate, nanoparticle concentration, and suspension stability, ensuring that the nanoparticles disperse uniformly and reach the contamination site with minimal clogging or retention.

To ensure reliable and reproducible results, column tests must be carefully designed, considering factors such as column size and the ratio of column length to diameter. Furthermore, the choice of medium (e.g., grain size, uniformity) affects nanoparticle mobility. A controlled and standardized medium allows for consistent results while flow rate and injection method should replicate natural groundwater flow as closely as possible to ensure realistic transport behavior.

By measuring nanoparticle concentration at various distances from the injection point, the tests help establish the radius of influence (ROI), which is essential for estimating the effective treatment zone and designing injection strategies to maximize remediation coverage.

By carefully planning and conducting transport tests, researchers can optimize the use of nanoparticles in remediation applications, ensuring their effectiveness while minimizing costs and environmental risks.

Besides considering transport phenomena for applications in nanoremediation, a specific focus was on a proper evaluation of the (eco)toxicological impact of specific nanoparticles (cellulose nanofibers), used as building blocks by POLIMI for the design of different families of new sorbent materials.

These studies were devoted to a proper eco-design of the nanostructured materials further applied for water treatment (see DV4.5.3). They consisted in both validating the building blocks (TEMPO-oxidized cellulose nanofibers, TOCNF) and the other components of final nanosponges' formulations and verifying the best operative conditions to ensure a safe use of the new nanostructured materials.

For these reasons, we evaluated the environmental safety of TOCNF by an acute *in vivo* study with marine mussels *Mytilus galloprovincialis* and sea urchins. Moreover, we optimized the nanostructured sorbent materials, obtained by promoting the cross-linking of TOCNF with branched polyethyleneimine, to prevent the release of toxic components in water and to preserve remediation efficiency by removal of heavy metal contaminants.

3. Table of contents

1. TECHNICAL REFERENCES	3
DOCUMENT HISTORY	4
2. ABSTRACT	6
3. TABLE OF CONTENTS	7
LIST OF FIGURES.....	7
4. TRANSPORT TESTS FOR NANOPARTICLE TRACKING	9
4.1 TRANSPORT TESTS FOR NANOPARTICLE TRACKING (POLITO).....	9
4.1.1 <i>Introduction.....</i>	9
4.1.2 <i>Methodologies.....</i>	10
4.1.3.1 <i>Set-up for non-magnetic particles.....</i>	13
4.1.3.2 <i>Set-up for magnetic particles.....</i>	14
4.1.3.3 <i>An example of nanoparticles transport test.....</i>	15
5. ECO-SAFETY AND FATE OF CELLULOSE NANOFIBERS	18
5.1 EVALUATION OF THE (ECO)TOXICOLOGICAL IMPACT OF CELLULOSE NANOFIBERS (POLIMI)	18
5.1.1 <i>Introduction.....</i>	18
5.1.2 <i>Methodologies.....</i>	19
5.1.3 <i>Results and Discussion.....</i>	20
5.1.4 <i>Conclusions.....</i>	22
5.2 OPTIMIZATION OF NANOSTRUCTURED SORBENT MATERIALS THROUGH THE REPRODUCTIVE TOXICITY ASSESSMENT OF CNS' BUILDING BLOCKS IN SEA URCHINS	22
5.2.1 <i>Introduction.....</i>	22
5.2.2 <i>Methodologies.....</i>	22
5.2.3 <i>Results and Discussion.....</i>	23
5.2.4 <i>Conclusions.....</i>	25
5.3 ECO-SAFETY ASSESSMENT OF NANOSTRUCTURED SORBENT MATERIALS ON SEA URCHINS	25
5.3.1 <i>Introduction.....</i>	25
5.3.2 <i>Methodologies.....</i>	26
5.3.3 <i>Results and Discussion.....</i>	27
5.3.4 <i>Conclusions.....</i>	29
6. CONCLUSIONS.....	30
7. REFERENCES	31

List of Figures

FIGURE 1: ONE PERISTALTIC PUMP (ON LEFT) AND ONE SCREW PUMP (ON RIGHT).....	11
FIGURE 2: SOME EXAMPLES OF COLUMN THAT CAN BE USED IN NANOPARTICLES TRANSPORT TEST. FROM SMALL SCALE PMMA COLUMN (INNER DIAMETER OF 1.6CM, PACKED LENGTH OF 18CM) ON LEFT, STAINLESS STEEL COLUMN (INNER DIAMETER 20CM, PACKED LENGTH OF 1M) ON CENTER AND LABORATORY PVC LYSIMETER (INNER DIAMETER 30CM, PACKED LENGTH 70CM)	12
FIGURE 3: SOME POROUS MEDIA MATERIALS. QUARTZ SAND ON LEFT AND GLASS BEADS ON RIGHT.....	12
FIGURE 4: THE DYNAMIC LIGHT SCATTERING DLS (A) AND THE SPECTROPHOTOMETER (B)	13
FIGURE 5: EXPERIMENTAL SET-UP FOR NON FERROMAGNETIC NANOPARTICLES TRANSPORT TEST	14

FIGURE 6: EXPERIMENTAL SET-UP FOR FERROMAGNETIC NANOPARTICLES TRANSPORT TEST	15
FIGURE 7: NANOPARTICLES INJECTED IN THE COLUMN TEST AFTER SCANNING ELECTRON MICROSCOPE (SEM) ANALYSIS	16
FIGURE 8: AN EXAMPLE OF BREAKTHROUGH CURVES FOR NANOPARTICLES	16
FIGURE 9: AN EXAMPLE OF VERTICAL PROFILE OF ATTACHED NANOPARTICLES OVER TIME	17
FIGURE 10. GRAPHICAL DESCRIPTION OF THE EXPERIMENTAL DESIGN OF THE ECOTOXICITY ASSESSMENT OF CNF AND TOCNF	20
FIGURE 11. LIGHT MICROSCOPY OF CNF AND TOCNF SUSPENSION IN THREE WATER MEDIA (80×). CNF NOT SONICATED AND SONICATED IN MILLIQ (A AND B), ASW (C	20
FIGURE 12. LIGHT MICROSCOPY OF CNF AND TOCNF IN HEMOLYMPH. HEMOCYTES STAINED WITH NEUTRAL RED (20×). (A) CNF (1 MG/L); (B) TOCNF (1 MG/L).....	21
FIGURE 13. CONCENTRATION-RESPONSE CURVES FOR BPEI ON EMBRYOTOXICITY, SPERMIOXICITY AND EGG TOXICITY TESTS WITH THE SEA URCHIN <i>P. LIVIDUS</i> AND <i>A. LIXULA</i> . IN THE GRAPHS, THE DASHED LINES INDICATE THE EC50. VALUES REPRESENTED THE MEAN OF TRIPLICATE EXPERIMENTS WITH ERROR BARS INDICATING THE STANDARD ERROR.....	24
FIGURE 14. SUPERIMPOSITION OF A) ¹ H NMR SPECTRUM OF REFERENCE BPEI AND B) ¹ H NMR SPECTRUM OF SEAWATER SAMPLE AFTER EXTRACTION PROCESS. IT IS POSSIBLE TO IDENTIFY BY COMPARISON OF SPECTRUM (B) WITH REFERENCE SPECTRUM (A) THE CHARACTERISTIC SIGNALS OF BPEI, CONFIRMING ITS PRESENCE IN THE EXTRACT FROM THE CNS LEACHATE.	25
FIGURE 15. EMBRYOTOXICITY OF CNS LEACHATE TO SEA URCHINS. FERTILIZED EGGS OF <i>P. LIVIDUS</i> AND <i>A. LIXULA</i> WERE EXPOSED FOR 48 H TO CNS LEACHATE SOLUTIONS, THEN, THE PERCENTAGE OF NORMAL EMBRYOS AT THE PLUTEUS STAGE WAS DETERMINED. RESULTS WERE REPORTED AS MEAN ± SE. STATISTICAL SIGNIFICANCE FOR EACH CONDITION <i>VS</i> CONTROL (0% CNS LEACHATE) IS INDICATED BY ASTERISK(S) (*P ≤ 0.05 AND **P ≤ 0.01).....	28
FIGURE 16. EGG MORPHOLOGY ASSESSMENT IN SEA URCHIN AFTER CNS LEACHATE EXPOSURE. SCANNING ELECTRON MICROGRAPHS OF SEA URCHIN EGGS UNEXPOSED (A) AND EXPOSED TO CNS LEACHATE SOLUTIONS (B, C, D). UNEXPOSED EGGS WERE ABOUT 100 μM IN DIAMETER AND SHOWED A ROUND SHAPE (A). EGG SIZE AND SHAPE WERE NOT AFFECTED BY CNS LEACHATE EXPOSURE (B, C, D). NEVERTHELESS, AFTER CNS LEACHATE 1 EXPOSURE, MATERIAL PARTICLES WERE FOUND ATTACHED TO THE EGG SURFACE (B), WHOSE QUANTITY PROGRESSIVELY DECREASED AFTER EXPOSURE TO CNS LEACHATE 2 (C) AND CNS LEACHATE 3 (D).....	29

4. Transport tests for nanoparticle tracking

4.1 Transport tests for nanoparticle tracking (PoliTO)

(Contributors: Rajandrea Sethi, Silvia Lupato, Monica Granetto, Marco Coha, Alessandro Casasso)

4.1.1 Introduction

Nanomaterials, with their distinctive properties, find applications across diverse fields, including catalysis, water treatment, energy storage, medicine, and agriculture. Their behavior significantly differs from the same materials at larger scales, primarily due to surface effects and quantum effects. These factors imbue nanomaterials with enhanced or novel mechanical, thermal, magnetic, electronic, optical, and catalytic properties (Joudeh and Linke, 2022).

Nanomaterials with larger surface areas and higher surface-to-volume ratios typically exhibit increased reactivity due to their expanded reaction surface making them a good candidate for pollutant remediation (Guerra et al., 2018). Contaminants can be remediated using nanomaterials through various mechanisms, including absorption, adsorption, chemical reactions, photocatalysis, and filtration and three primary types of nanomaterials used for such purposes, namely inorganic, carbon-based, and polymer-based materials can be identified (Mauter and Elimelech, 2008; Tong et al., 2012; Zhao et al., 2011).

At laboratory scale nanoparticle characterization involves a variety of techniques used to analyse their physical and chemical properties, including their size, morphology, surface charge, and composition (Mourdikoudis et al., 2018). The more common methods used in nanoparticle characterization are listed below:

- UV-Visible Spectroscopy is based on the principle of surface plasmon resonance (SPR) and is used to study the optical properties and to determine nanoparticles concentration in liquid media
- Brunauer–Emmett–Teller (BET) method is based on the adsorption and desorption principle developed by Stephen Brunauer, Paul Emmett, and Edward Teller, and it is considered one of the best methods for the analysis of NP surface area.
- X-Ray Diffraction XRD is used to determine the crystalline structure and phase of nanoparticles, providing insight into their crystal arrangement and purity.
- X-ray photoelectron spectroscopy (XPS) This technique is considered the most sensitive approach for the determination of NP exact elemental ratios, chemical state, and exact bonding nature of NP materials. XPS is based on the photoelectric effect that can identify the elements within a material, or covering a material, as well as their chemical state with high precision
- Fourier Transform Infrared Spectroscopy FTIR helps to identify the functional groups present on the surface of nanoparticles by analyzing their interaction with infrared light.
- Atomic Force Microscopy AFM provides high-resolution imaging of nanoparticle surface topography, allowing for the measurement of size, shape, and surface roughness.
- Scanning Electron Microscopy SEM offers detailed images of nanoparticle morphology and surface structure by scanning the sample with a focused electron beam.
- Transmission Electron Microscopy TEM provides high-resolution imaging of nanoparticle internal structure and morphology at the nanoscale level, enabling detailed analysis of shape, size, and crystallinity.
- Dynamic Light Scattering DLS and Nanoparticle tracking analysis (NTA) are used to measure the size distribution of nanoparticles in suspension by analysing the scattering of light or the individual positional changes of the particles caused by Brownian motion.

These methods, often used in combination, provide comprehensive insights into the characteristics of nanoparticles, which are critical for applications in fields such as pollutant remediation but also drug delivery, catalysis, and materials science.

In designing and investigating an effective remediation intervention using nanoparticles, it is essential to study the mechanisms governing their transport in both the unsaturated and saturated phases (Tosco et al., 2014). Column experiments, offering precise control over environmental variables and boundary conditions, are highly effective for simulating the dynamic conditions of aquifers in a near-natural state within a laboratory environment (Sethi and Di Molfetta, 2019). Consequently, they are extensively used to studying the transport mechanisms and eventual fate of engineered nanoparticles (ENPs). In these tests, a fundamental aspect is the measurement of nanoparticle concentrations at the column outlet and those attached to the porous medium at various distances from the injection point. These two datasets, when combined, allow for the determination of the interaction mechanisms between the nanoparticles and the porous medium, the radius of influence covered by the nanoparticles, and the overall mass balance.

According to literature review, nanoparticle concentration in liquid media can be measured using various techniques, each offering specific advantages depending on the type of nanoparticles and the required accuracy..

1. Dynamic light scattering (DLS) is a common method that measures the size distribution of nanoparticles by analyzing the fluctuations in scattered light caused by their Brownian motion. From this data, concentration can be estimated using appropriate models.
2. Another widely used technique is nanoparticle tracking analysis (NTA), which visualizes and tracks the motion of individual nanoparticles using a laser-based optical system. This provides both size distribution and concentration data by directly counting the particles.
3. UV-visible spectroscopy can also be used to measure concentration by analyzing the light absorption characteristics of nanoparticles, which are typically correlated with their optical properties.
4. Gravimetric methods, on the other hand, involve separating the nanoparticles from the liquid media (e.g., via centrifugation or filtration) and measuring their total mass.

Other more complex technique includes tuneable resistive pulse sensing (TRPS), a method that involves passing nanoparticles through a nanopore. Changes in electrical resistance caused by the particles blocking the pore are used to determine their size and concentration. Similarly, nanoparticle flow cytometry (nFCM) analyzes scattered light and fluorescence signals from nanoparticles as they flow through a laser beam. This high-throughput method provides sensitive and accurate measurements of concentration across a wide range of nanoparticle types. For metallic nanoparticles, inductively coupled plasma mass spectrometry (ICP-MS) is often employed. This highly sensitive technique dissolves the nanoparticles and measures their elemental composition to determine concentration.

Each of these methods has its own strengths and limitations. For instance, DLS and NTA are well-suited for colloidal nanoparticles and easy to use, while ICP-MS excels in analyzing metallic nanoparticles. The choice of technique depends on the specific properties of the nanoparticles and the level of detail required.

In this study, specific column experimental setups have been developed, differentiated for the injection of non-magnetic and magnetic nanoparticles. Among the various techniques available for determining nanoparticle concentration in both liquid and solid phases, the most rapid methods were selected, given the high number of analyses performed, while maintaining a high degree of sensitivity.

4.1.2 Methodologies

All experiments aimed at evaluating column transport of a nanosuspension or a contaminant share the use of several common components:

- One injection system. Injecting a nanosuspension into a column requires precise control over flow rates to ensure consistent delivery and accurate simulation of transport processes. The choice of pump depends on factors such as the nanoparticle suspension's viscosity, required flow rate, column

resistance, and experiment duration. Various types of pumps can be used for this purpose, each with specific advantages depending on the experimental setup and requirements. The **peristaltic pumps** that operate by compressing a flexible tube with rotating rollers to push fluid forward, are ideal for precise flow control and suitable for low-viscosity nanoparticle suspensions. **Syringe pumps** use a motor-driven piston to push fluid from a syringe at a controlled flow rate. They provide a very accurate flow rates, even at micro- or nanoscale and are ideal for small volumes and highly controlled experiments. When higher volume needs to be injected a **diaphragm pumps**, that use a flexible diaphragm driven by a motor to create suction and push fluid forward, can be used. When a highly viscous nanosuspension must be injected a **screw pump** can be a versatile option. It operates based on the principle of rotating one or more screws to move fluid along a helical path. Also, **piston pumps** can be used for the same purpose.



Figure 1: One peristaltic pump (on left) and one screw pump (on right)

- At least one column. When designing column transport tests for nanoparticles, the choice of column material and type plays a critical role in ensuring accurate, reproducible results (Lewis and Sjöstrom, 2010). The selected material must be chemically inert, mechanically stable, and compatible with the nanoparticles and experimental conditions. **Polymethylmethacrylate (PMMA)** columns allow for visual observation of fluid and nanoparticle movement and are ideal for low-pressure experiments while **Polyvinyl Chloride (PVC)** can be used for constructing large-scale columns and is suitable for low-cost studies. **Teflon (PTFE)** is recommended for experiments involving harsh chemicals or highly reactive nanoparticles and for long-term studies requiring minimal material degradation. **Glass** columns are chemically inert, ensuring no interaction with nanoparticle suspensions. Therefore, it is excellent for visual monitoring of flow patterns even after multiple applications. Lastly **stainless steel** can be used for high-pressure column tests and in studies involving reactive nanoparticles like zero-valent iron (nZVI) under extreme conditions.

The ratio of column length to column diameter (L/D) in transport tests is a critical parameter that influences the flow dynamics and data quality. The choice of this ratio depends on the purpose of the experiment, the scale of the study, and the characteristics of the porous media and nanoparticles. Low L/D ratio (from 5:1 to 10:1) refers to easier to set up and maintain system and require less experimental material but they may introduce edge effects and boundary artifacts, reducing the accuracy of transport parameter estimations.



Figure 2: Some examples of column that can be used in nanoparticles transport test. From small scale PMMA column (inner diameter of 1.6cm, packed length of 18cm) on left, stainless steel column (inner diameter 20cm, packed length of 1m) on center and laboratory PVC lysimeter (inner diameter 30cm, packed length 70cm)

- Packing material. **Quartz sand or glass beads** generally offer a controlled and homogeneous environment, which facilitates consistent and reproducible results. Such standardization isolates the behavior of nanoparticles from the variability inherent in **natural soils**, making it easier to interpret and compare experimental data (Naka et al., 2016). In fact, **Natural Soils** provides a more realistic simulation of natural environments but introduces variability. Lastly **synthetic porous media** are engineered materials, such as sintered glass or ceramic, offering consistent properties



Figure 3: Some porous media materials. Quartz sand on left and glass beads on right

- A nanosuspension stirring system. It is crucial to maintain a uniform and stable suspension during experiments. Nanoparticles in fact tend to aggregate due to their small size and high surface energy, so proper stirring ensures consistent distribution and prevents settling. The suspensions need to be continuously stirred at a rate from 200 to 1000 rpm. Different type of stirrer can be used, from **magnetic stirrer**, not suitable for high-viscosity solutions, ferromagnetic suspension and larger volumes to **ultrasonic stirring** or **high-shear mixers**.

- An analytical instrument for nanoparticles quantification. As stated in the previous chapter, techniques such as dynamic light scattering DLS and UV-Vis can be preferred due to their faster and low-cost analysis compared to other methods.

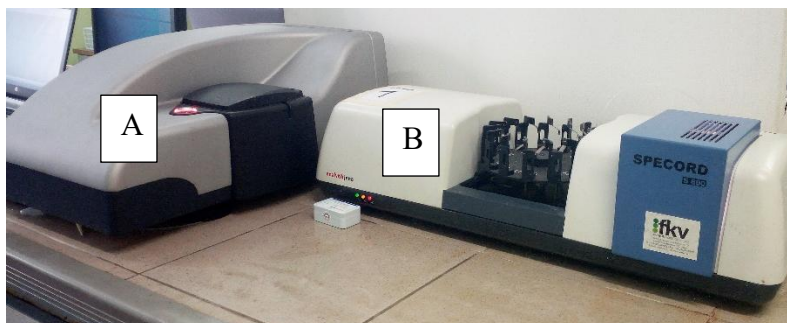


Figure 4: The dynamic light scattering DLS (A) and the spectrophotometer (B)

In this project two different setup for nanoparticles transport and tracking tests has been developed, one for nonmagnetic nanoparticles, the other for ferromagnetic ones.

4.1.3 Results and discussion

4.1.3.1 Set-up for non-magnetic particles

Among the different nonferromagnetic nanoparticles that can be used for contaminated sites remediation silica based, carbon-based and polymer-based nanomaterial can be listed (Del Prado-Audelo et al., 2021). Unlike magnetic nanoparticles, these materials rely on chemical reactivity, adsorption, or catalytic activity rather than magnetic separation for their environmental applications.

In this experimental setup, the nanoparticle suspension is kept in suspension using a magnetic or shaft stirrer and is injected directly into the column through an injection system. For low-viscosity suspensions, a peristaltic pump is typically used, while a different system is chosen for viscous suspensions. The concentrations at the column outlet are monitored using a UV-Vis spectrophotometer (Specord s600, Analytic Jena) connected inline with the column, with a minimum measurement interval of 10 seconds. Outlet samples from the spectrophotometer, as well as inlet samples, can also be analysed using DLS (Zetasizer, Malvern Panalytical) to determine both particle concentration and size distributions.

To obtain spatial profiles at the end of the test, it is necessary to unpack the column in different fractions of the porous medium collected at various depths and perform a detachment of the attached particles. This can be achieved by placing different aliquots of the porous medium in deionized water and sonicating them for a fixed time. The resulting suspension is then characterized in term of nanoparticles concentration measured using again the spectrophotometer.

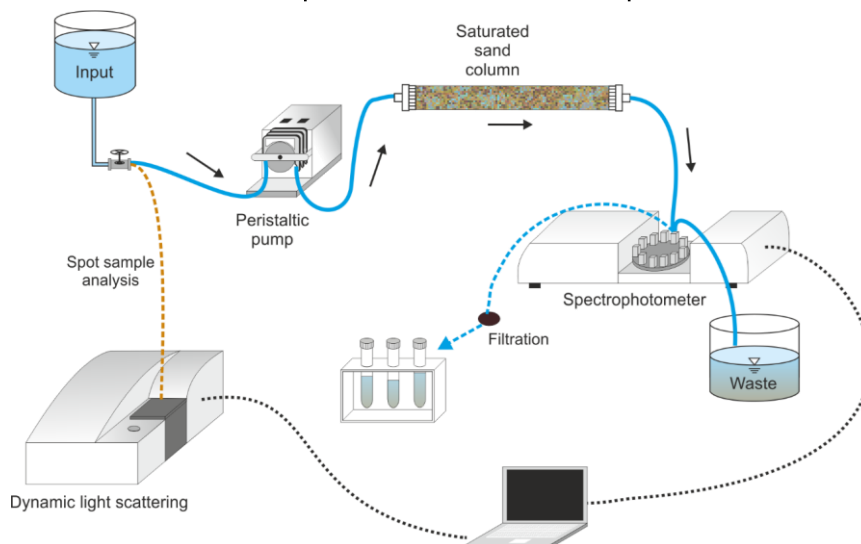


Figure 5: Experimental set-up for non ferromagnetic nanoparticles transport test

The injection protocol involved the following steps (Granetto et al., 2022; Tosco et al., 2009):

1. Columns were pre-conditioned with background solution (deionized water/tap water/buffered water) for 5 pore volumes PVs (obtained from theoretical calculation).
2. A tracer (generally a NaCl or KBr salt) was injected and the outlet tracer concentration monitored with the spectrophotometer at a wavelength of 198.5nm. From the obtained breakthrough curve, an estimation of the real pore volume can be obtained.
3. Background solution was injected for at least 5 PVs,
4. Nanoparticles were injected for at least 10PVs
5. Background solution was injected for at least 5 PVs
6. A subsequent flushing for other 5 PVs or more could be performed to understand the possible detachment of particles from the porous media due to changing in solution ionic strength and pH.

From these column tests, breakthrough curves and spatial deposition profiles of the nanoparticles can be determined. Additionally, through a modelling process, the governing parameters of the interaction mechanism between the porous medium and nanoparticles can be identified.

4.1.3.2 Set-up for magnetic particles

The same injection protocol can be applied to magnetic particles, such as zero-valent iron particles or other metallic particles (Tiraferri and Sethi, 2009; Vecchia et al., 2009). However, the experimental setup requires the use of a non-magnetic stirrer to prevent the particles from aggregating on the magnets or other components of the stirrer. The measurement of particle concentrations in both the solid and liquid phases is carried out using a magnetic susceptibility meter (Bartington MS2 susceptibility meter). Magnetic susceptibility measurements were performed to monitor changes in oscillator frequency, reflecting variations in the magnetic susceptibility of the model porous medium. The ferromagnetic susceptibility was recorded using a resonant circuit with a constant capacitance, where the coil's inductance varied according to the surrounding susceptibility.

In particular, in order to determine the vertical profile of attached nanoformulation the scanning process began at the top of the column for calibration purposes, with the detector moving downward and subsequently measuring every centimetre for 5 seconds as it moved upward. Initially, background measurements were acquired through multiple scans of the saturated column.

Processing the raw frequency data involved three main steps:

- (i) subtracting background noise and correcting for temperature-induced signal drift,
- (ii) deconvoluting the data to isolate the elementary iron signal by solving a set of linear equations for the deconvolved frequencies, and
- (iii) converting the deconvolved frequencies into ferromagnetic concentrations using specific conversion constants previously determine starting from suspension of nanoparticles at known concentration

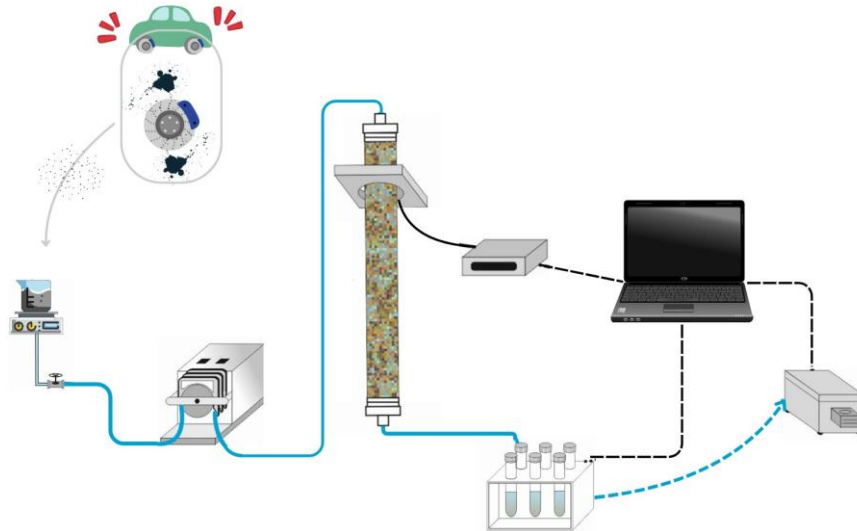


Figure 6: Experimental set-up for ferromagnetic nanoparticles transport test

4.1.3.3 An example of nanoparticles transport test

Transport data from column experiments, when integrated with mass balance calculations and numerical simulations, enable the determination of key transport parameters, including attachment efficiency, maximum migration distance, deposition coefficient, and maximum nanoparticle concentration in the solid phase (Wang et al., 2024). This comprehensive approach provides a precise evaluation of nanoparticle mobility.

In this last section a brief example of ferromagnetic nanoparticles transport tests results is reported. The injection of a iron oxide nanoparticles (Figure 7) has been performed in a Plexiglass column with an internal diameter of 16mm and a total packed length of 17.5cm. The injected flow rate was 1 ml/min. The liquid sample at the outlet of the column has been measured for magnetic susceptibility every 0.3PV. After each injection phase the vertical profile of magnetic susceptibility has been measured moving downward each 2 cm along the column.

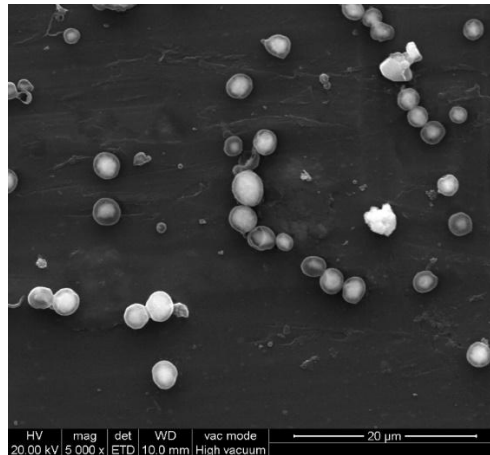


Figure 7: Nanoparticles injected in the column test after scanning electron microscope (SEM) analysis

A breakthrough curve is one of the most important results that can be obtained from a column test. In details a breakthrough curve plots the concentration of a substance in the liquid effluent (C) over time or pore volumes (V), normalized by the initial input concentration (C_0). Usually, it is a graphical representation used to describe the transport and release of contaminants or substances from a solid phase into a liquid phase under specific flow conditions. It is essential for understanding the dynamics of leaching processes, the mobility of substances, and the interaction between the leaching medium and the solid material. Understanding breakthrough curves in leaching tests is critical for designing and optimizing remediation strategies, predicting contaminant fate in subsurface environments, and evaluating material performance under field-like conditions.

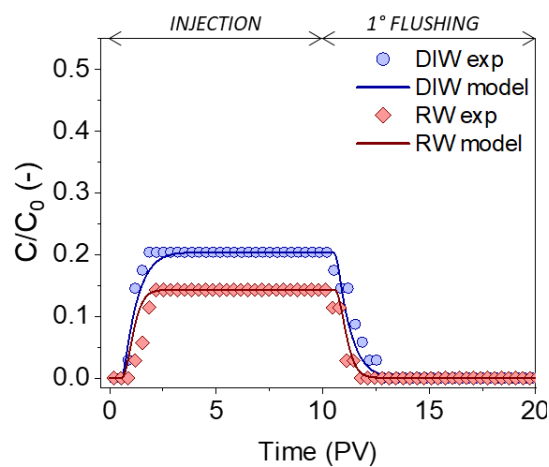


Figure 8: An example of breakthrough curves for nanoparticles

Lastly, the nanoparticles vertical profile can be determined. The vertical profile of nanoparticles in a column test provides critical insights into the spatial distribution of nanoparticles along the length of the column after injection. This profile helps evaluate how nanoparticles interact with the porous medium, their deposition behavior, and the extent of transport or retention within the system.

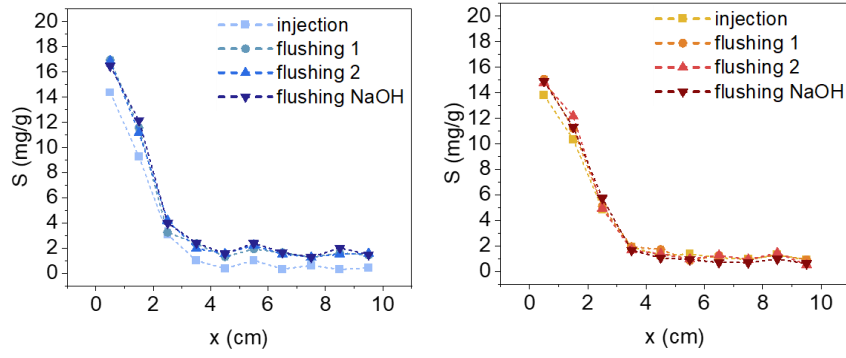


Figure 9: An example of vertical profile of attached nanoparticles over time

5. Eco-safety and fate of cellulose nanofibers

5.1 Evaluation of the (eco)toxicological impact of cellulose nanofibers (PoliMI)

(Contributors: Laura Riva, Carlo Punta (PoliMI) and Ilaria Corsi (UniSI))

The increasing industrial application of nanocellulose (NC) and its potential release into aquatic environments necessitate a thorough assessment of its environmental safety and ecotoxicity. In this study (Rusconi et al., 2024), we evaluated two types of cellulose nanofibers, non-oxidized (CNF) and TEMPO-oxidized (TOCNF), through acute in vivo experiments using the marine bivalve *Mytilus galloprovincialis*. We tested concentrations of 1 µg/L and 1 mg/L to simulate realistic and severe exposure scenarios, respectively. Our findings revealed that TOCNF exhibited better dispersion in natural seawater (NSW) than CNF, likely due to electrostatic repulsion between its negatively charged surface groups and interactions with colloidal organic matter.

Using labeled stocks, we detected both fiber types within mussel tissues, specifically in the gills and hemolymph. We observed sub-lethal biological responses, including destabilization of hemocyte lysosomal membranes and inhibition of P-glycoprotein (P-gp) efflux activity in the gills. CNF showed stronger inhibitory effects at the highest concentration (1 mg/L). Furthermore, we detected inhibition of cholinergic enzymes (ASCh–ChE) in hemocytes, gills, and digestive glands, regardless of fiber oxidation state or concentration. Conversely, we did not observe significant effects on oxidative stress markers or biotransformation processes in the digestive glands and gills. Overall, our results demonstrate that NC uptake can disrupt gill and immune cell functionality through mechanical interactions, even under environmentally realistic exposure scenarios, highlighting the need to incorporate safety considerations into future risk assessments.

5.1.1 Introduction

Cellulose is a naturally abundant biopolymer primarily derived from plants and biomass, with a market projected to reach \$300 million by 2026 (Barhoum et al., 2020). Nanocellulose (NC), characterized by at least one dimension below 100 nm, possesses unique physicochemical properties, including high crystallinity, low density, and high biodegradability (Dufresne, 2013). These characteristics make NC increasingly relevant across multiple sectors, including biomedicine, the food industry, construction, and environmental remediation (Thomas et al., 2018).

CNF are the most widely used NC materials and are typically produced via top-down processes from biomass (Gallo Stampino et al., 2021; Akatan et al., 2022). Standard CNF are obtained through enzymatic-mediated pre-hydrolysis, whereas TOCNF are produced by converting alcoholic groups into carboxylic moieties, resulting in a distinct surface chemistry (Pääkko et al., 2007; Pierre et al., 2017). As production volumes continue to increase, significant environmental release is anticipated, requiring accurate evaluations of both human and environmental safety. Although probabilistic modeling currently suggests a low risk for European surface waters, the rapid global expansion of NC applications calls for updated and comprehensive risk assessments (Shatkin & Kim, 2015).

Human toxicity studies have yielded controversial findings. Some evidence suggests that CNF may be more toxic than cellulose nanocrystals in lung cells, potentially due to their elongated fibrous morphology (Endes et al., 2016). Fiber dimensions, particularly length and diameter, are critical parameters influencing biological interactions and toxicological outcomes (Farcas et al., 2016). Studies on aquatic organisms remain limited. While research on zebrafish and *Daphnia* species indicates low acute toxicity, sub-lethal effects on growth and reproduction have been reported (Harper et al., 2016). Importantly, there remains a significant knowledge gap regarding marine species. The frequent detection of natural textile fibers, such as cotton and wool, in marine organisms, sometimes at higher frequencies than synthetic fibers, raises concerns about the potential risks associated with nanoscale cellulose. In this context, we aimed to address these gaps by investigating NC uptake and associated biological effects, including neurotoxicity and oxidative stress, in *M. galloprovincialis*.

5.1.2 Methodologies

The methodologies employed in this study were categorized into material synthesis, physical-chemical characterization, and *in vivo* biological assessments using the marine mussel *Mytilus galloprovincialis* (Figure 10).

Synthesis of Nanocellulose and Labeled Stocks

We synthesized two types of nanocellulose from cotton linter sheets. CNF were produced through enzymatic-mediated pre-hydrolysis using Endoglucanase FiberCare R, followed by refining and high-pressure homogenization. TOCNF were synthesized *via* TEMPO-mediated oxidation of cellulose pulp using KBr and NaClO, with the pH maintained between 10.5 and 11. To track fiber uptake, Rhodamine B-labeled versions (CNF–RhB and TOCNF–RhB) were created through a multi-step process involving silanization with APTES and EDC/NHS coupling.

Physico-chemical Characterization

The fibers were characterized using several techniques:

- **Chemical composition:** Solid-phase FTIR spectra identified functional groups, such as the carboxyl signal at 1722 cm^{-1} unique to TOCNF.
- **Surface charge:** The point of zero charge (pH_{PZC}) was measured using the pH drift method, and Zeta potential was determined via Dynamic Light Scattering (DLS) in both MilliQ and natural seawater (NSW).
- **Crystallinity:** Powder XRD patterns were recorded, and the Crystallinity Index (CrI) was calculated using the Segal method.
- **Morphology:** Transmission Electron Microscopy (TEM) and light microscopy were used to observe fiber dimensions and aggregation in MilliQ, artificial seawater (ASW), and NSW. Sonication was applied to mimic natural breakdown processes like wave motion.

Experimental Design and *In Vivo* Exposure

Mussels were acclimatized in NSW before being divided into five experimental groups: a control and four exposure groups (CNF and TOCNF at $1\text{ }\mu\text{g/L}$ and 1 mg/L).

- **Uptake Study (96 h):** Mussels were exposed to RhB-labeled fibers to track tissue distribution in the hemolymph, gills, and mantle using fluorescence microscopy.
- **Acute Toxicity Test (48 h):** Mussels were exposed to unlabeled fibers to evaluate sub-lethal biological responses.

Biological Responses (Biomarkers)

A battery of assays was performed to evaluate the impact of nanocellulose:

- **Cytotoxicity:** The Neutral Red Retention Time (NRRT) assay assessed the stability of lysosomal membranes in circulating hemocytes.
- **Efflux Activity:** A P-glycoprotein (P-gp) efflux assay was conducted on gill biopsies using Rhodamine B as a substrate and verapamil as a positive inhibitor.
- **Biochemical Assays:** Enzymatic activities were measured in the gills and digestive glands, including cholinesterase (ASCh–ChE) for neurotoxicity and several markers for oxidative stress and detoxification (CAT, GST, GR, GPx, and LPO). Statistical analysis was performed using one-way ANOVA and Bonferroni multiple comparison tests.

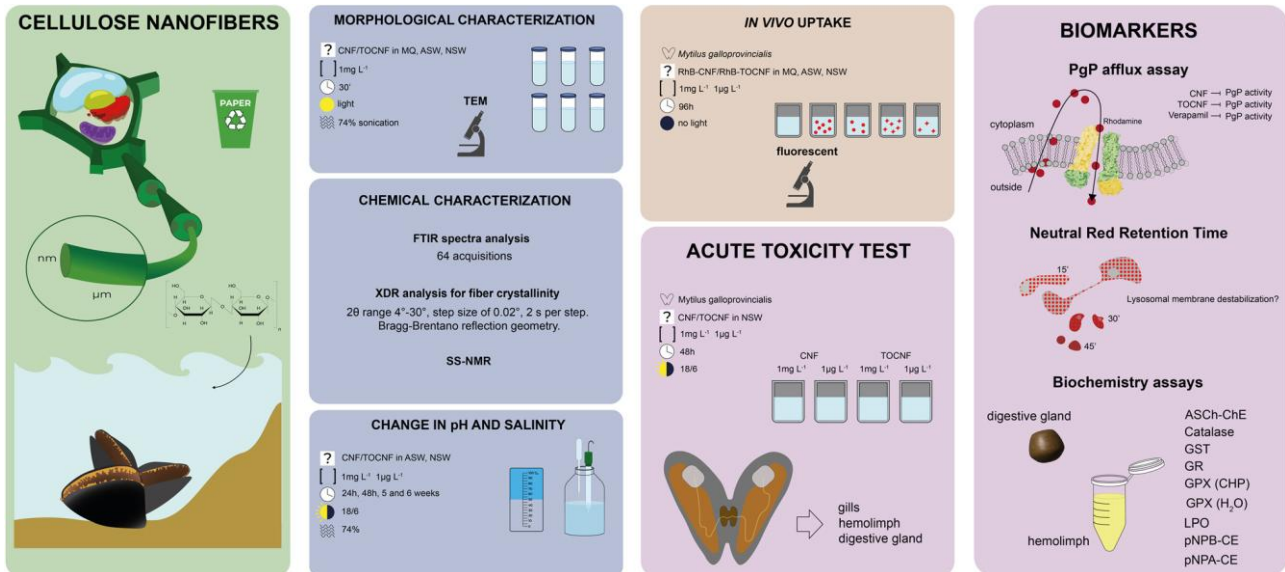


Figure 10. Graphical description of the experimental design of the ecotoxicity assessment of CNF and TOCNF.

5.1.3 Results and Discussion

Physico-chemical Behavior in Seawater

The two nanocellulose types exhibited distinct chemical properties: TOCNF possessed carboxylic moieties (identified by an FTIR signal at 1722 cm^{-1}), while CNF featured only hydroxyl groups. Consequently, TOCNF was more negatively charged at neutral pH ($\text{pH}_{\text{PZC}} 4.01$) compared to the nearly neutral CNF ($\text{pH}_{\text{PZC}} 7.10$). While both maintained nanometric diameters across all water media, their aggregation patterns differed significantly in natural seawater (NSW). Sonication, mimicking natural wave action, caused nano-defibrillation and greater dispersion of TOCNF, likely due to electrostatic repulsion between negative surface charges and interactions with colloidal organic matter. In contrast, CNF formed smaller but more condensed aggregates (Figure 11).

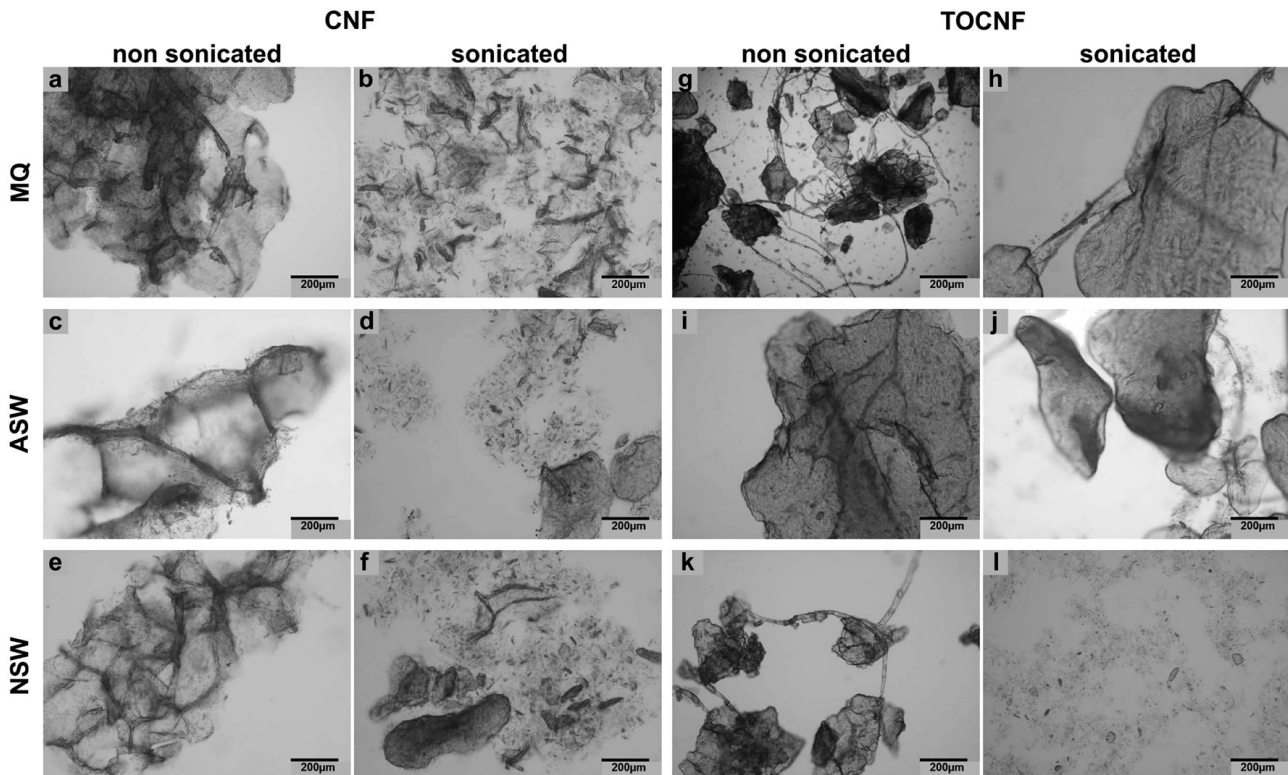


Figure 11. Light microscopy of CNF and TOCNF suspension in three water media (80×). CNF not sonicated and sonicated in MilliQ (a and b), ASW (c and d) and NSW (e and f). TOCNF not sonicated and sonicated in MilliQ (g and h).

h), ASW (i and j) and NSW (k and l).

Uptake and Tissue Distribution

Fluorescence microscopy confirmed the uptake of labeled CNF in the gills and hemolymph at both realistic (1 $\mu\text{g/L}$) and acute (1 mg/L) concentrations. Individual TOCNF fibers were less visible, which we attributed to their high state of dispersion (nano-defibrillation) in NSW. Notably, hemocytes were observed adhering to and surrounding the fibers in the circulatory fluid, providing evidence of a direct cellular immune response.

Biological and Ecotoxicological Effects

The study identified three primary areas of sub-lethal impact:

- **Immune System Disruption:** Both fibers caused significant destabilization of hemocyte lysosomal membranes, even at the lowest concentration of 1 $\mu\text{g/L}$. At the 1 mg/L dose, CNF showed a more prolonged destabilizing effect compared to TOCNF.
- **Gill Functionality:** Both NC types significantly inhibited P-glycoprotein (P-gp) efflux activity in the gills. At the higher concentration, this inhibition was three times stronger than that of the standard inhibitor verapamil, suggesting a severe compromise of the mussels' multi-xenobiotic resistance.
- **Neurotoxicity:** Cholinergic (ASCh–ChE) activities were inhibited across the hemolymph, gills, and digestive glands, with TOCNF generally exerting a stronger inhibitory effect than CNF. Conversely, we found no significant impact on oxidative stress (LPO) or biotransformation enzymes (GST) in the digestive gland, indicating that the fibers did not trigger traditional biochemical defense pathways within the 48-hour timeframe.

Mechanism and Environmental Significance

We suggest that these toxicological effects are driven by mechanical and physical interactions with cell membranes rather than direct biochemical binding. For instance, P-gp inhibition likely results from membrane disruption or ATP depletion caused by fiber adhesion. The relative lack of response in the digestive gland compared to the gills and hemolymph suggests that the short 48-hour exposure may have limited the translocation of fibers to deeper metabolic organs (**Figure 12**).

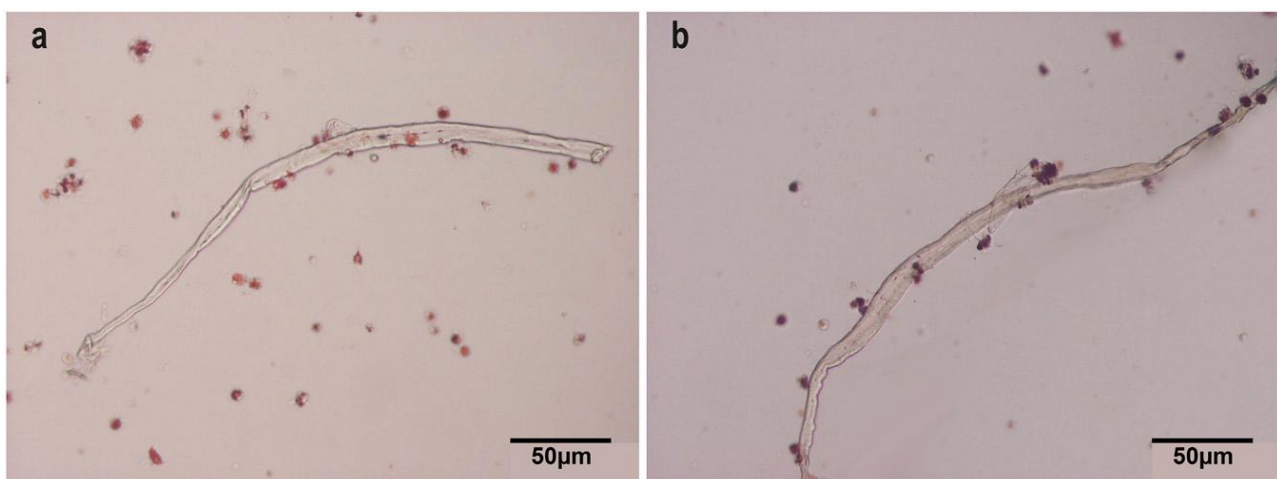


Figure 12. Light microscopy of CNF and TOCNF in hemolymph. Hemocytes stained with neutral red (20 \times). (a) CNF (1 mg/L); (b) TOCNF (1 mg/L).

Ultimately, these findings are of high ecological relevance because they demonstrate that nanocellulose can impair immune regulation and gill function at environmentally realistic concentrations (1 $\mu\text{g/L}$), necessitating its inclusion in future marine risk assessments.

5.1.4 Conclusions

Cellulose nanofibers (CNF and TOCNF) disrupt mussel immune regulation, gill functionality, and cholinergic systems at environmentally realistic concentrations. These impacts primarily result from mechanical interactions with cell membranes. Although no acute mortality or oxidative stress was observed within 48 hours, these sub-lethal effects necessitate comprehensive future risk assessments.

5.2 Optimization of nanostructured sorbent materials through the reproductive toxicity assessment of CNS' building blocks in sea urchins

(Contributors: Laura Riva, Carlo Punta (PoliMI) and Ilaria Corsi (UniSI))

Using a safe-by-design approach, in this study (Esposito et al., 2024) we evaluated the reproductive toxicity of nanostructured cellulose sponge components on sea urchins. Branched polyethylenimine (bPEI) was identified as the most toxic constituent, impairing gamete physiology, fertilization, and embryo development in *Arbacia lixula* and *Paracentrotus lividus*. Our proposed safety protocol of consecutive leaching treatments successfully minimizes these environmental risks while preserving the sponge's sorbent efficacy for marine pollution remediation.

5.2.1 Introduction

In the framework of a safer-by-design approach, we engineered nanostructured cellulose sponges (CNS) for marine remediation with the goal of assessing their environmental safety alongside their performance prior to market application (Corsi et al., 2018; Corsi et al., 2023). During safety evaluations, concerns emerged regarding potential reproductive effects in marine organisms, plausibly linked to the release of unreacted chemical additives used during sponge synthesis.

CNS are produced through a two-step process: first, the preparation of TOCNF, followed by cross-linking with bPEI and citric acid (CA) (Fiorati et al., 2020). Although TOCNF is a bio-based material often considered inherently safe, its nanoscale dimensions warrant dedicated ecotoxicological assessment, particularly in marine environments where data remain scarce (Fen et al., 2022). bPEI, a synthetic cationic polymer widely used for heavy metal adsorption, raises additional safety questions due to its limited toxicological characterization in marine species (Kunath et al., 2003). Likewise, CA is generally regarded as a low-concern compound, yet its potential effects on sensitive early life stages of marine organisms have been largely overlooked (Singh Dhillon et al., 2011).

In this study, we addressed these knowledge gaps by individually evaluating TOCNF, bPEI, and CA on the reproduction of the Mediterranean Sea urchins *Paracentrotus lividus* and *Arbacia lixula* (Singh Dhillon et al., 2011). These species serve as valuable model organisms due to the high sensitivity of their early developmental stages to environmental stressors. Moving beyond conventional embryotoxicity assays, we adopted a multi-response integrated approach, assessing gamete quality parameters, such as motility, mitochondrial activity, and intracellular reactive oxygen species (ROS) levels, together with fertilization success and developmental competence (Gallo et al., 2022). This strategy provides a comprehensive evaluation of the potential risks that individual CNS components may pose to marine ecosystems.

5.2.2 Methodologies

The methodologies for this study focused on individually screening the building block components of CNS to identify the specific drivers of ecotoxicity in marine environments.

1. Preparation of Test Solutions

We evaluated three main constituents of CNS by preparing stock solutions in double distilled water or filtered natural seawater (FNSW):

- **bPEI:** A 25 kDa stock solution was filtered and diluted in FNSW to concentrations ranging from 0.01 to 1000 µg/mL, with pH adjusted to 8.1.
- **Citric Acid:** A stock solution was diluted to final concentrations of 0.01 to 1000 µg/mL.
- **TOCNF:** Produced *via* the TEMPO/NaClO/NaBr oxidation system, TOCNF was stirred in FNSW and filtered to create test solutions between 0.01 and 1000 µg/mL.

2. Biological Models and Gamete Collection

Adult sea urchins of two species, *Paracentrotus lividus* and *Arbacia lixula*, were collected from the Gulf of Naples. We induced spawning through the injection of 0.5 M KCl, collecting eggs in FNSW and spermatozoa "dry" directly from the gonopores. Only high-quality gametes were selected for subsequent testing after preliminary checks.

3. Ecotoxicological Bioassays

We employed a multi-response integrated approach consisting of three primary bioassays:

- **Embryotoxicity Test:** Fertilized eggs were exposed to the test solutions for 48 hours to determine the percentage of normally developed plutei larvae.
- **Spermioxicity Bioassay:** Spermatozoa were exposed to test solutions for one hour before being used to fertilize untreated eggs; we measured the fertilization rate (FR) at the zygote or 2-cell stage.
- **Egg Toxicity Bioassay (Ovotoxicity):** In this innovative test, we exposed unfertilized eggs to the components for one hour before adding untreated spermatozoa to evaluate female gamete fertilization competence.

4. Assessment of Gamete Quality

To understand the physiological mechanisms of toxicity, we evaluated several parameters using fluorescent staining and spectroscopy:

- **Mitochondrial Membrane Potential (MMP):** Measured using the mitochondrial dye JC-1.
- **Oxidative Status:** We estimated intracellular ROS levels with H2DCFDA and superoxide anions with DHE.
- **Intracellular pH (pH_i):** Evaluated using the cell-permeant dye BCECF-AM.
- **Sperm Motility:** Assessed through visual estimation by an expert operator using a sperm counting chamber under 40X magnification.

5. Leachate Characterization and Statistics

To confirm the presence of chemical additives, the CNS leachate was freeze-dried and characterized using ¹H NMR and elemental analysis to identify signals characteristic of bPEI. Statistical significance was determined using one-way ANOVA, and EC50 values were calculated using concentration-response curves.

5.2.3 Results and Discussion

Our results identify bPEI as the primary driver of ecotoxicity in CNS. Among the three tested components, bPEI was the most toxic, severely impairing embryo development, fertilization rates, and gamete physiology in both species.

In male gametes, bPEI exposure significantly reduced sperm motility while increasing MMP and intracellular ROS levels. We hypothesize that bPEI inhibits ATP synthase, leading to energy imbalance and oxidative stress. In female gametes, bPEI also increased MMP and likely induced membrane damage or phospholipid rearrangement, generating surface aggregates that physically hinder sperm binding (**Figure 13**).

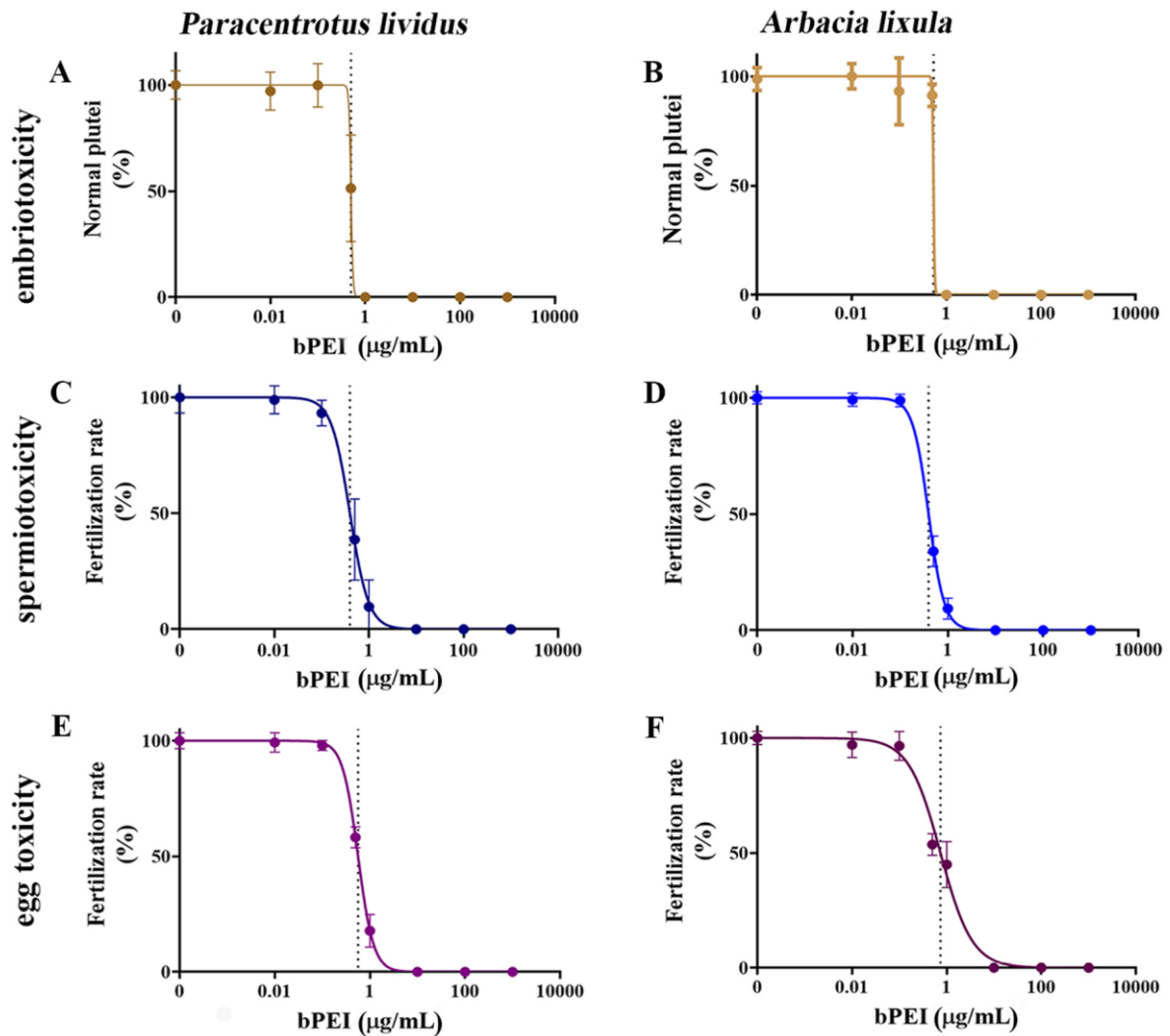


Figure 13. Concentration-response curves for bPEI on embryotoxicity, spermotoxicity and egg toxicity tests with the sea urchin *P. lividus* and *A. lixula*. In the graphs, the dashed lines indicate the EC₅₀. Values represented the mean of triplicate experiments with error bars indicating the standard error.

CA primarily affected embryo development, with one species (EC₅₀ = 5.7 µg/mL) markedly more sensitive than the other (EC₅₀ = 107.2 µg/mL). This embryotoxicity is likely due to chelation of essential ions such as Ca²⁺ and Mg²⁺, which are crucial for gastrulation and skeletogenesis. In contrast, TOCNF showed the lowest risk, affecting development only at concentrations (100–1000 µg/mL) far above predicted environmental levels.

¹H NMR (**Figure 14**) and elemental analysis confirmed that bPEI is released from CNS into seawater.

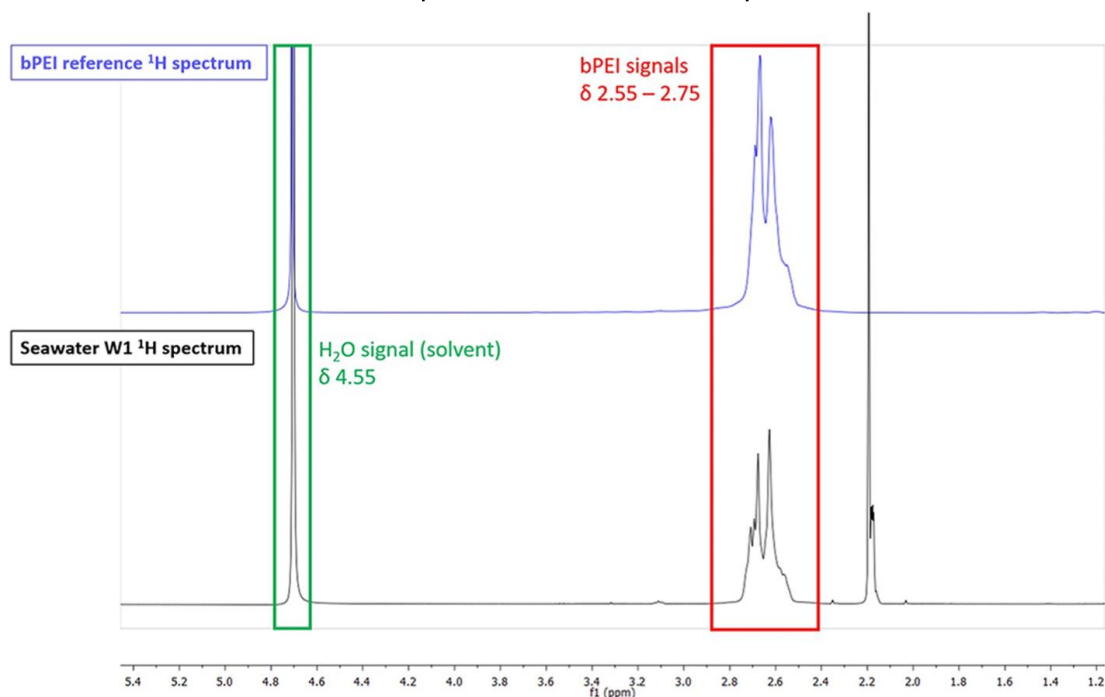


Figure 14. Superimposition of a) ^1H NMR spectrum of reference bPEI and b) ^1H NMR spectrum of seawater sample after extraction process. It is possible to identify by comparison of spectrum (b) with reference spectrum (a) the characteristic signals of bPEI, confirming its presence in the extract from the CNS leachate.

These findings establish a clear cause–effect relationship between bPEI leaching and reproductive impairment.

We demonstrate that a multi-leaching safety protocol effectively removes excess, unreacted bPEI, ensuring CNS environmental safety while preserving adsorption efficiency.

5.2.4 Conclusions

Concluding, bPEI is the primary driver of ecotoxicity in CNS, leaching into seawater and impairing sea urchin reproduction. However, a safer-by-design multi-leaching protocol effectively removes excess bPEI, reducing hazardous levels for marine organisms without compromising adsorption efficiency or structural integrity. These results confirm that conditioned CNS are environmentally benign and suitable for sustainable marine remediation applications.

5.3 Eco-safety assessment of nanostructured sorbent materials on sea urchins

(Contributors: Laura Riva, Carlo Punta (PoliMI) and Ilaria Corsi (UniSI))

In this study (Esposito et al., 2023), after the eco-toxicological assessment of the CNS' building blocks, identifying bPEI as the driver of ecotoxicity, we evaluated the eco-safety of CNS leachate on sea urchin reproduction. Our results show that the leachate impairs gamete quality, fertilization success, and embryo development, likely due to the presence of synthesis additives. However, we found that consecutive leaching and seawater conditioning eliminate the observed toxicity while preserving decontamination efficiency, thereby enabling the development of a safe and effective remediation protocol.

5.3.1 Introduction

Marine environmental pollution is a critical global issue affecting biodiversity and has driven the development of nanoremediation as a sustainable solution. Although nano-structured materials (NMs) offer clear advantages over traditional technologies, their practical application remains limited because their

environmental fate and safety are still not fully understood (Esposito et al., 2021). To address these concerns, we shifted our focus toward bio-based NMs, specifically nanocellulose derived from sustainable plant sources. Nanocellulose is biodegradable, cost-effective, and exhibits superior adsorption capacity for chemical contaminants compared to its macroscale counterparts (Trache et al., 2020).

Within this class of materials, nanostructured CNS have demonstrated high efficiency in removing heavy metals and organic pollutants from both freshwater and seawater (Fiorati et al., 2020; Melone et al., 2015; Riva et al., 2020). In our preliminary eco-safety assessments on marine microalgae and mussels, we observed sub-lethal effects, including reduced growth and destabilization of immune cells, which highlighted the need for more rigorous evaluation. In this study, we aimed to support the safe in-situ application of CNS by assessing the impact of its leachate on the reproduction of two sea urchin species, *Paracentrotus lividus* and *Arbacia lixula*.

Sea urchins represent ideal biological models for ecotoxicity studies because they are benthic organisms and their early life stages are highly sensitive to contaminants (Bellas et al., 2008). While spermotoxicity and embryotoxicity assays are standardized for *P. lividus*, we also investigated *A. lixula* as a potential alternative model species in light of the recent population declines observed in *P. lividus* (Guidetti, 2004). Furthermore, we introduced an innovative ovotoxicity assay to evaluate the fertilization competence of female gametes. By integrating these bioassays with a detailed characterization of gamete quality parameters, including motility, mitochondrial activity, and intracellular reactive oxygen species (ROS) levels, we provide a comprehensive and integrated framework for reproductive risk assessment.

5.3.2 Methodologies

The methodology of this study focused on evaluating the reproductive safety of nanostructured CNS leachates using a multi-response approach involving two sea urchin species.

1. Synthesis of CNS and Leachate Preparation

The CNS was synthesized from cotton linter cellulose through TOCNF. These were cross-linked using 25 KDa bPEI and CA. The final material was freeze-dried, heated, and ground into a powder.

To simulate remediation conditions we prepared three consecutive leachates:

- **CNS-1:** 1.25 g of CNS powder was stirred in 1 L of FNSW for 2 hours and filtered.
- **CNS-2 and CNS-3:** The recovered powder from the previous step was re-exposed to fresh FNSW to produce subsequent leaching stages. Both undiluted (100%) and scalar dilutions (ranging from 0.3% to 50%) of these leachates were tested.

2. Adsorption Efficiency Tests

We verified if the multi-leaching process impacted the material's decontamination performance by testing the Zn(II) removal efficiency of both fresh CNS and the recovered CNS-3 powder using ICP-OES analysis.

3. Biological Models and Gamete Collection

The study utilized two sea urchin species: *Paracentrotus lividus* and *Arbacia lixula*. Gamete spawning was induced via 0.5 M KCl injection, and only high-quality gametes, determined by egg roundness and sperm motility, were used for the experiments.

4. Ecotoxicological Bioassays

Three primary bioassays were performed to assess reproductive success:

- **Embryotoxicity Test:** Fertilized eggs (zygotes) were exposed to leachates for 48 hours to determine the percentage of normal plutei larvae.
- **Spermotoxicity Test:** Spermatozoa were exposed to leachates for 1 hour before being used to fertilize untreated eggs to calculate the fertilization rate (FR).

- **Ovotoxicity Test (Innovative):** Developed by the research group, this test involved exposing eggs to leachates for 1 hour before fertilization with untreated sperm to evaluate female gamete competence.

5. Gamete Quality and Physiological Assessment

To identify the mechanisms behind the observed toxicity, we evaluated several physiological parameters:

- **Sperm Motility:** Evaluated via visual estimation under a microscope.
- **Mitochondrial Activity:** Measured as mitochondrial membrane potential (MMP) using the JC-1 fluorescent dye.
- **Oxidative Status:** Intracellular levels of hydrogen peroxide and superoxide ions were measured using H2DCF-DA and DHE fluorochromes.
- **Intracellular pH (pH_i):** Determined using the ratiometric pH indicator BCECF-AM.
- **Morphological Assessment:** Gamete structure and potential fiber entanglement were examined using Scanning Electron Microscopy (SEM).

6. Statistical Analysis

Data were analyzed for normality and variance homogeneity before undergoing one-way ANOVA and Fisher's LSD test. The No-Observed-Effect Concentration (NOEC) was determined using Dunnett's test

5.3.3 Results and Discussion

The results of the study demonstrate that nanostructured CNS leachates significantly impact sea urchin reproduction in a concentration-dependent manner. In both *P. lividus* and *A. lixula*, undiluted leachates (CNS-1, 2, and 3) led to a total absence of normal plutei larvae and severely impaired the fertilizing capability of both male and female gametes (**Figure 15**).

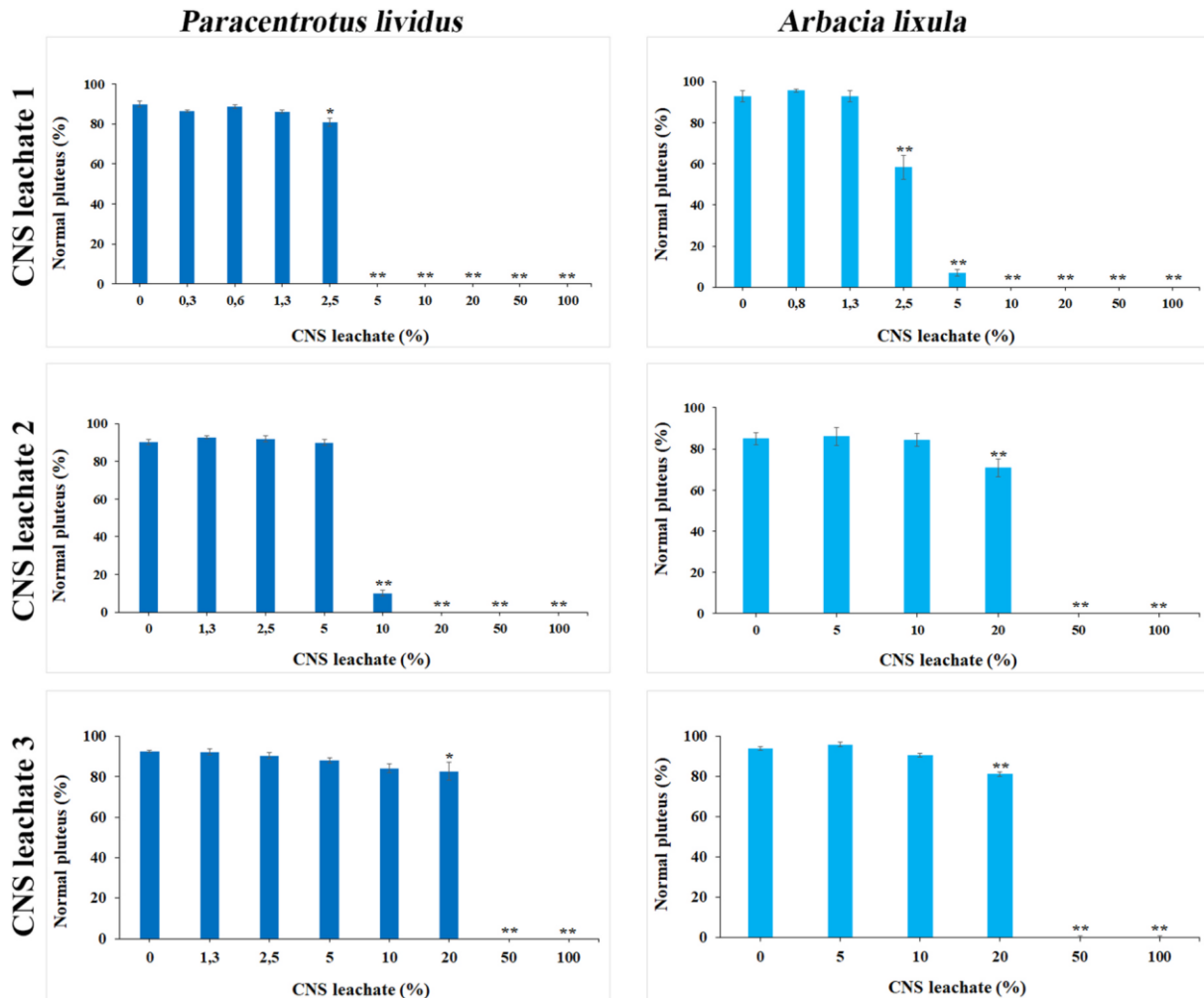


Figure 15. Embryotoxicity of CNS leachate to sea urchins. Fertilized eggs of *P. lividus* and *A. lixula* were exposed for 48 h to CNS leachate solutions, then, the percentage of normal embryos at the pluteus stage was determined. Results were reported as mean \pm SE. Statistical significance for each condition vs control (0% CNS leachate) is indicated by asterisk(s) (* $P \leq 0.05$ and ** $P \leq 0.01$).

Physiological assessments revealed that the first leachate (CNS-1) was the most toxic, reducing sperm motility and increasing mitochondrial membrane potential (MMP) and reactive oxygen species (ROS) levels. The FNSW s hypothesize that high MMP triggers excessive ROS production, leading to oxidative damage that compromises sperm fitness. While SEM analysis showed no structural damage to the gametes, undiluted leachates caused significant spermatozoa entanglement and the attachment of material particles to the egg surfaces. This physical interference likely prevents proper sperm-egg binding, contributing to the observed drop in fertilization rates.

The observed ecotoxicity is primarily attributed to the leaching of chemical additives used during CNS synthesis, such as bPEI and citric acid. To address this, we evaluated a multi-leaching protocol to "condition" the material. They found that while toxicity significantly decreased by the third leaching stage (CNS-3), especially when combined with dilution, the material's ability to remove heavy metals remained robust. Specifically, the Zn(II) adsorption efficiency only slightly decreased from approximately 45% to 38%, a difference deemed irrelevant for practical remediation applications.

The results also confirm that *A. lixula* is a suitable alternative to the increasingly scarce *P. lividus* for marine ecotoxicity testing. Overall, the study highlights that through an eco-design approach, involving consecutive leaching and seawater conditioning, CNS can be rendered safe for marine applications without sacrificing its decontamination performance (Figure 16).

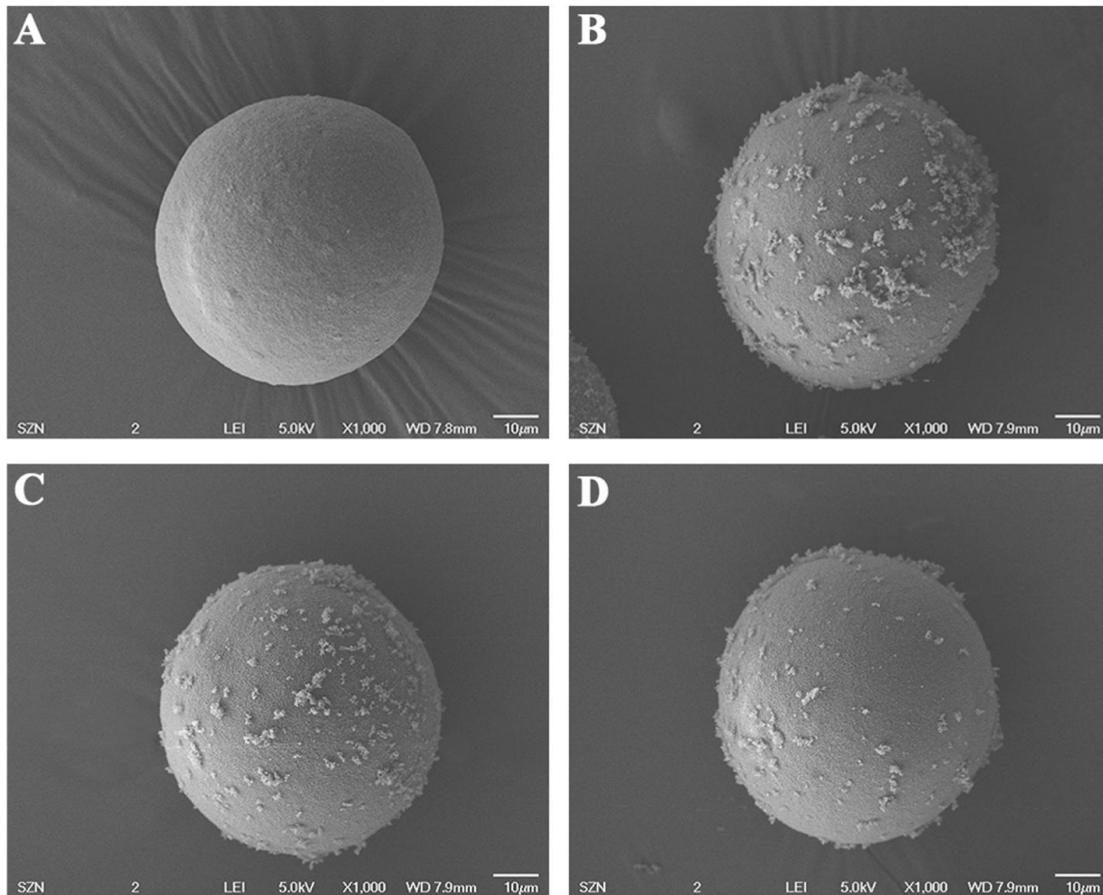


Figure 16. Egg morphology assessment in sea urchin after CNS leachate exposure. Scanning electron micrographs of sea urchin eggs unexposed (A) and exposed to CNS leachate solutions (B, C, D). Unexposed eggs were about 100 μm in diameter and showed a round shape (A). Egg size and shape were not affected by CNS leachate exposure (B, C, D). Nevertheless, after CNS leachate 1 exposure, material particles were founded attached to the egg surface (B), whose quantity progressively decreased after exposure to CNS leachate 2 (C) and CNS leachate 3 (D).

5.3.4 Conclusions

We employed sea urchin gamete and embryo bioassays, including an innovative ovotoxicity test, to evaluate the environmental safety of CNS leachates for seawater remediation. Exposure impaired fertilization competence and embryo development in *Paracentrotus lividus* and *Arbacia lixula*, supporting the latter as a potential alternative ecotoxicological model. Mechanistically, leachate increased ROS production in sperm, reducing motility and fertilizing capacity, while eggs showed enhanced mitochondrial activity to maintain metabolic balance. Multi-leaching and dilution treatments effectively reduced toxicity, improving CNS safety for environmental applications.

6. Conclusions

Nanomaterials exhibit unique physicochemical properties that make them highly effective in various applications, including pollutant remediation. Their high surface-to-volume ratio and enhanced reactivity enable multiple remediation mechanisms such as adsorption, photocatalysis, and chemical transformation. The selection of suitable nanomaterials, whether inorganic, carbon-based, or polymer-based—depends on the specific environmental challenge and desired interaction mechanism. They can be used directly in nano-remediation processes or can be considered valuable building blocks for the design of nanostructured systems to be used for soil and water treatment. In both cases, the final fate of nanosized materials should be considered and deeply investigated.

Characterization techniques play a crucial role in understanding nanomaterials' properties, ensuring their effective application in remediation. Methods such as UV-Vis spectroscopy, X-ray diffraction, dynamic light scattering, and electron microscopy provide comprehensive insights into nanoparticles' size, morphology, composition, and surface chemistry. These analytical approaches, often used in combination, allow for precise control over nanoparticle formulation and behavior in experimental and real-world conditions.

Transport studies are essential for assessing the fate and mobility of nanoparticles in porous media, particularly in groundwater remediation. Column experiments offer a controlled environment to simulate subsurface conditions and study nanoparticle transport dynamics. The choice of experimental setup, including column material, injection system, and analytical techniques, directly influences the accuracy and reproducibility of the results. In this study, different setups were developed for non-magnetic and magnetic nanoparticles, with rapid and sensitive quantification methods employed to ensure high-throughput analysis.

Breakthrough curves and vertical deposition profiles obtained from column tests provide valuable insights into nanoparticle mobility, interaction with the porous medium, and transport parameters such as attachment efficiency and deposition coefficients. By integrating experimental data with numerical modeling, the mechanisms governing nanoparticle transport and retention can be better understood, ultimately contributing to the optimization of nanomaterial-based remediation strategies.

Moreover, final fate also implies an in-depth investigation of the eco-safety of the nanomaterials used in water treatment. Ecotoxicological evaluation in simulated real scenarios represents a valuable tool to support the eco-design of safe and sustainable nanostructured materials for environmental remediation since the early stage of their production at lab scale. The results obtained within this project support the use of nanocellulose and derived materials in water treatment systems.

As nanotechnology continues to evolve, further research is needed to enhance the efficiency, scalability, and environmental fate investigation of nanomaterials.

7. References

- Akatan, K., Kabdrakhmanova, S., Kuanyshbekov, T., Ibraeva, Z., Battalova, A., Joshy, K. S., & Thomas, S. (2022). Highly-efficient isolation of microcrystalline cellulose and nanocellulose from sunflower seed waste via environmentally benign method. *Cellulose*, 29(7), 3787–3802. <https://doi.org/10.1007/s10570-022-04527-4>
- Barhoum, A., Jeevanandam, J., Rastogi, A., Samyn, P., Boluk, Y., Dufresne, A., Danquah, M. K., & Bechelany, M. (2020). Plant celluloses, hemicelluloses, lignins, and volatile oils for the synthesis of nanoparticles and nanostructured materials. *Nanoscale*, 12(45), 22845–22890. <https://doi.org/10.1039/d0nr04795c>
- Bellas, J., Saco-Álvarez, L., Nieto, Ó., & Beiras, R. (2008). Ecotoxicological evaluation of polycyclic aromatic hydrocarbons using marine invertebrate embryo-larval bioassays. *Marine Pollution Bulletin*, 57(6–12), 493–502. <https://doi.org/10.1016/j.marpolbul.2008.02.039>
- Corsi, I., Venditti, I., Trotta, F., & Punta, C. (2023). Environmental safety of nanotechnologies: The eco-design of manufactured nanomaterials for environmental remediation. In *Science of the Total Environment* (Vol. 864, Number July 2022). <https://doi.org/10.1016/j.scitotenv.2022.161181>
- Corsi, I., Winther-Nielsen, M., Sethi, R., Punta, C., Della Torre, C., Libralato, G., Lofrano, G., Sabatini, L., Aiello, M., Fiordi, L., Cinuzzi, F., Caneschi, A., Pellegrini, D., & Buttino, I. (2018). Ecofriendly nanotechnologies and nanomaterials for environmental applications: Key issue and consensus recommendations for sustainable and ecosafe nanoremediation. *Ecotoxicology and Environmental Safety*, 154, 237–244. <https://doi.org/10.1016/j.ecoenv.2018.02.037>
- Del Prado-Audelo, M.L., García Kerdan, I., Escutia-Guadarrama, L., Reyna-González, J.M., Magaña, J.J., Leyva-Gómez, G., 2021. Nanoremediation: Nanomaterials and Nanotechnologies for Environmental Cleanup. *Frontiers in Environmental Science* 9.
- Dhillon, G. S., Brar, S. K., Verma, M., & Tyagi, R. D. (2011). Recent Advances in Citric Acid Bio-production and Recovery. In *Food and Bioprocess Technology* (Vol. 4, Number 4, pp. 505–529). <https://doi.org/10.1007/s11947-010-0399-0>
- Dufresne, A. (2013). Nanocellulose: A new ageless bionanomaterial. *Materials Today*, 16(6), 220–227. <https://doi.org/10.1016/j.mattod.2013.06.004>
- Endes, C., Camarero-Espinosa, S., Mueller, S., Foster, E. J., Petri-Fink, A., Rothen-Rutishauser, B., Weder, C., & Clift, M. J. D. (2016). A critical review of the current knowledge regarding the biological impact of nanocellulose. In *Journal of Nanobiotechnology* (Vol. 14, Number 1). BioMed Central Ltd. <https://doi.org/10.1186/s12951-016-0230-9>
- Esposito, M. C., Corsi, I., Russo, G. L., Punta, C., Tosti, E., & Gallo, A. (2021). The era of nanomaterials: A safe solution or a risk for marine environmental pollution? *Biomolecules*, 11(3), 1–25. <https://doi.org/10.3390/biom11030441>
- Esposito, M. C., Riva, L., Russo, G. L., Punta, C., Corsi, I., Tosti, E., & Gallo, A. (2024). Reproductive toxicity assessment of cellulose nanofibers, citric acid, and branched polyethylenimine in sea urchins: Eco-design of nanostructured cellulose sponge framework (Part B). *Environmental Pollution*, 350, 123934. <https://doi.org/10.1016/j.envpol.2024.123934>
- Esposito, M. C., Russo, G. L., Riva, L., Punta, C., Corsi, I., Tosti, E., & Gallo, A. (2023). Nanostructured cellulose sponge engineered for marine environmental remediation: Eco-safety assessment of its leachate on sea urchin reproduction (Part A). *Environmental Pollution*, 334(July), 122169. <https://doi.org/10.1016/j.envpol.2023.122169>
- Farcas, M. T., Kisin, E. R., Menas, A. L., Gutkin, D. W., Star, A., Reiner, R. S., Yanamala, N., Savolainen, K., & Shvedova, A. A. (2016). Pulmonary exposure to cellulose nanocrystals caused deleterious effects to reproductive system in male mice. *Journal of Toxicology and Environmental Health - Part A: Current Issues*, 79(21), 984–997. <https://doi.org/10.1080/15287394.2016.1211045>
- Fen, L. B., Kamaldin, J., & Pengiran, H. (2022). An overview of cellulose nanofiber physicochemical characterizations and biological studies in relation to nanosafety concerns. In *Industrial Applications of Nanocellulose and its Nanocomposites* (pp. 245–261). Elsevier. <https://doi.org/10.1016/B978-0-323-89909-3.00009-2>
- Fiorati, A., Grassi, G., Graziano, A., Liberatori, G., Pastori, N., Melone, L., Bonciani, L., Pontorno, L., Punta, C., & Corsi, I. (2020). Eco-design of nanostructured cellulose sponges for sea-water

- decontamination from heavy metal ions. *Journal of Cleaner Production*, 246, 119009. <https://doi.org/10.1016/j.jclepro.2019.119009>
- Gallo Stampino, P., Riva, L., Punta, C., Elegir, G., Bussini, D., & Dotelli, G. (2021). Comparative Life Cycle Assessment of Cellulose Nanofibres Production Routes from Virgin and Recycled Raw Materials. *Molecules*, 9(26), 2558. <https://doi.org/10.3390/molecules26092558>
- Gallo, A., Esposito, M. C., Boni, R., & Tosti, E. (2022). Oocyte quality assessment in marine invertebrates: a novel approach by fluorescence spectroscopy. *Biological Research*, 55(1). <https://doi.org/10.1186/s40659-022-00403-4>
- Granetto, M., Serpella, L., Fogliatto, S., Re, L., Bianco, C., Vidotto, F., Tosco, T., 2022. Natural clay and biopolymer-based nanopesticides to control the environmental spread of a soluble herbicide. *SCIENCE OF THE TOTAL ENVIRONMENT* 806. <https://doi.org/10.1016/j.scitotenv.2021.151199>
- Guerra, F.D., Attia, M.F., Whitehead, D.C., Alexis, F., 2018. Nanotechnology for Environmental Remediation: Materials and Applications. *Molecules* 23. <https://doi.org/10.3390/molecules23071760>
- Harper, B. J., Clendaniel, A., Sinche, F., Way, D., Hughes, M., Schardt, J., Simonsen, J., Stefaniak, A. B., & Harper, S. L. (2016). Impacts of chemical modification on the toxicity of diverse nanocellulose materials to developing zebrafish. *Cellulose*, 23(3), 1763–1775. <https://doi.org/10.1007/s10570-016-0947-5>
- Joudeh, N., Linke, D., 2022. Nanoparticle classification, physicochemical properties, characterization, and applications: a comprehensive review for biologists. *Journal of Nanobiotechnology* 20, 262. <https://doi.org/10.1186/s12951-022-01477-8>
- Kunath, K., Von Harpe, A., Fischer, D., Petersen, H., Bickel, U., Voigt, K., & Kissel, T. (2003). Low-molecular-weight polyethylenimine as a non-viral vector for DNA delivery: Comparison of physicochemical properties, transfection efficiency and in vivo distribution with high-molecular-weight polyethylenimine. *Journal of Controlled Release*, 89(1), 113–125. [https://doi.org/10.1016/S0168-3659\(03\)00076-2](https://doi.org/10.1016/S0168-3659(03)00076-2)
- Lewis, J., Sjöström, J., 2010. Optimizing the experimental design of soil columns in saturated and unsaturated transport experiments. *Journal of Contaminant Hydrology* 115, 1–13. <https://doi.org/10.1016/j.jconhyd.2010.04.001>
- Mauter, M.S., Elimelech, M., 2008. Environmental Applications of Carbon-Based Nanomaterials. *Environ. Sci. Technol.* 42, 5843–5859. <https://doi.org/10.1021/es8006904>
- Melone, L., Rossi, B., Pastori, N., Panzeri, W., Mele, A., & Punta, C. (2015). TEMPO-Oxidized Cellulose Cross-Linked with Branched Polyethyleneimine: Nanostructured Adsorbent Sponges for Water Remediation. *ChemPlusChem*, 80(9), 1408–1415. <https://doi.org/10.1002/cplu.201500145>
- Mourdikoudis, S., Pallares, R.M., Thanh, N.T.K., 2018. Characterization techniques for nanoparticles: comparison and complementarity upon studying nanoparticle properties. *Nanoscale* 10, 12871–12934. <https://doi.org/10.1039/C8NR02278J>
- Naka, A., Yasutaka, T., Sakanakura, H., Kalbe, U., Watanabe, Y., Inoba, S., Takeo, M., Inui, T., Katsumi, T., Fujikawa, T., Sato, K., Higashino, K., Someya, M., 2016. Column percolation test for contaminated soils: Key factors for standardization. *Journal of Hazardous Materials* 320, 326–340. <https://doi.org/10.1016/j.jhazmat.2016.08.046>
- Pääkko, M., Ankerfors, M., Kosonen, H., Nykänen, A., Ahola, S., Österberg, M., Ruokolainen, J., Laine, J., Larsson, P. T., Ikkala, O., & Lindström, T. (2007). Enzymatic hydrolysis combined with mechanical shearing and high-pressure homogenization for nanoscale cellulose fibrils and strong gels. *Biomacromolecules*, 8(6), 1934–1941. <https://doi.org/10.1021/bm061215p>
- Pierre, G., Punta, C., Delattre, C., Melone, L., Dubessay, P., Fiorati, A., Pastori, N., Galante, Y. M., & Michaud, P. (2017). TEMPO-mediated oxidation of polysaccharides: An ongoing story. *Carbohydrate Polymers*, 165, 71–85. <https://doi.org/10.1016/j.carbpol.2017.02.028>
- Riva, L., Pastori, N., Panozzo, A., Antonelli, M., & Punta, C. (2020). Nanostructured Cellulose-Based Sorbent Materials for Water Decontamination from Organic Dyes. *Nanomaterials*, 10(8), 1570. <https://doi.org/10.3390/nano10081570>
- Rusconi, T., Riva, L., Punta, C., Montserrat, S., & Corsi, I. (2024). Environmental safety of nanocellulose: an in vivo acute study with marine mussels *Mytilus galloprovincialis*. *Environmental Science: Nano*. <https://doi.org/10.1039/D3EN00135K>
- Sethi, R., Di Molfetta, A., 2019. GROUNDWATER ENGINEERING A Technical Approach to Hydrogeology, Contaminant Transport and Groundwater Remediation. <https://doi.org/10.1007/978-3-030-20516-4>

- Shatkin, J. A., & Kim, B. (2015). Cellulose nanomaterials: life cycle risk assessment, and environmental health and safety roadmap. *Environmental Science: Nano*, 2(5), 477–499. <https://doi.org/10.1039/c5en00059a>
- Thomas, B., Raj, M. C., Athira, B. K., Rubiyah, H. M., Joy, J., Moores, A., Drisko, G. L., & Sanchez, C. (2018). Nanocellulose, a Versatile Green Platform: From Biosources to Materials and Their Applications. *Chemical Reviews*, 118, 11575–11625. <https://doi.org/10.1021/acs.chemrev.7b00627>
- Tiriferri, A., Sethi, R., 2009. Enhanced transport of zerovalent iron nanoparticles in saturated porous media by guar gum. *Journal of Nanoparticle Research* 11, 635–645. <https://doi.org/10.1007/s11051-008-9405-0>
- Tong, H., Ouyang, S., Bi, Y., Umezawa, N., Oshikiri, M., Ye, J., 2012. Nano-photocatalytic Materials: Possibilities and Challenges. *Advanced Materials* 24, 229–251. <https://doi.org/10.1002/adma.201102752>
- Tosco, T., Papini, M.P., Viggì, C.C., Sethi, R., 2014. Nanoscale zerovalent iron particles for groundwater remediation: a review. *J Clean Prod J Clean Prod* 77, 10–21.
- Tosco, T., Tiriferri, A., Sethi, R., 2009. Ionic Strength Dependent Transport of Microparticles in Saturated Porous Media: Modeling Mobilization and Immobilization Phenomena under Transient Chemical Conditions. *Environ. Sci. Technol.* 43, 4425–4431. <https://doi.org/10.1021/es900245d>
- Trache, D., Tarchoun, A. F., Derradji, M., Hamidon, T. S., Masruchin, N., Brosse, N., & Hussin, M. H. (2020). Nanocellulose: From Fundamentals to Advanced Applications. In *Frontiers in Chemistry* (Vol. 8, Number May). <https://doi.org/10.3389/fchem.2020.00392>
- Vecchia, E.D., Luna, M., Sethi, R., 2009. Transport in Porous Media of Highly Concentrated Iron Micro- and Nanoparticles in the Presence of Xanthan Gum. *Environ. Sci. Technol.* 43, 8942–8947. <https://doi.org/10.1021/es901897d>
- Wang, M., Bai, Y., Zuo, Q., Hu, H., 2024. Comparison of engineered nanoparticle transport in columns of three different lengths: Transport experiments and multi-observation point modeling. *Science of The Total Environment* 954, 176195. <https://doi.org/10.1016/j.scitotenv.2024.176195>
- Zhao, X., Lv, L., Pan, B., Zhang, W., Zhang, S., Zhang, Q., 2011. Polymer-supported nanocomposites for environmental application: A review. *Chemical Engineering Journal* 170, 381–394. <https://doi.org/10.1016/j.cej.2011.02.071>